Supporting Online Material for

A Neural Mechanism for Microsaccade Generation in the Primate Superior Colliculus

Ziad M. Hafed,* Laurent Goffart, Richard J. Krauzlis

*To whom correspondence should be addressed. E-mail: zhafed@salk.edu

Published 13 February 2009, *Science* **323**, 940 (2009)
DOI: 10.1126/science.1166112

This PDF file includes:

Supporting Online Material for:

"A Neural Mechanism for Microsaccade Generation in the Primate Superior Colliculus"

Z. M. Hafed, L. Goffart, & R. J. Krauzlis

Materials and Methods

Animal preparation. We recorded from two (J and W) adult rhesus monkeys (*Macaca mulatta*) that were 10–11 years of age and weighed 15–16 kg. We performed inactivation on monkey W and a third monkey (A; age: 10 years; weight: 12 kg) that was not used for the recording experiments. The monkeys were prepared using standard surgical techniques described in detail previously (*S1*). All experimental protocols were approved by the Institutional Animal Care and Use Committee and complied with United States Public Health Service policy on the humane care and use of laboratory animals. The laboratory setup for behavioral control and monitoring was identical to that described in (S*1*,*S2*).

Behavioral tasks. During recording, monkeys fixated a small, stationary spot presented at eye-level directly in front of them at the center of a CRT display. The fixation spot consisted of a single pixel of background luminance surrounded by a 1-pixel-thick white square. With our display geometry and distance, this 3x3 pixel stimulus corresponded to ~9x9 min arc of visual angle. Each fixation trial lasted for 3,500 ms, and we collected 9-140 fixation trials per neuron (mean 82.5 +/- 25.5 s.d.).

The monkeys also performed memory-guided and delayed visually-guided saccade tasks, as well as a fixation-blink task (described in refs. *S2*-*S5*). In the fixation-blink task, the monkeys were shown a stationary fixation spot at the center of the display and were given 500 ms to establish fixation on this spot. At the end of this 500-ms interval, the fixation spot disappeared for 500 ms and then reappeared for another 500 ms. The monkeys were required to maintain fixation throughout the blink interval and the subsequent interval after the fixation spot had reappeared. We collected 35-45 trials per neuron in this condition.

During inactivation, the monkeys fixated the same spot for 1,500-2,500 ms, before the spot was blanked for 200 ms and then reappeared randomly at one of four possible peripheral locations: 12^{o} to the right, left, up, or down. Upon reappearance of the peripheral spot, the monkeys were required to initiate a saccade to its location. Note that in the fixation interval that we analyzed (see below), there were no other visual stimuli on the display except the fixation spot, and the monkeys were not pre-cued to the location of the upcoming peripheral target. Thus, the fixation interval was not associated with any sustained attention or saccade preparation towards a particular

peripheral location. We collected 48 trials before muscimol injection (baseline) and 48 trials after (inactivation).

Single-neuron recording. We used tungsten microelectrodes (impedances: 900kΩ–1.7MΩ) to record extracellular action potentials of individual neurons in the deep layers of the SC (1.5–2.9 mm below surface). We mapped the response field of each neuron using a delayed visually-guided saccade task (*S2*,*S3*,*S5*), the data from which was also used for comparing the microsaccade-related activity to the activity associated with voluntary saccades.

Neurons (N = 54) were recorded from the rostral pole of the SC, representing foveal and parafoveal retinotopic locations (i.e. locations within 3 degrees of the center of the visual field). Neurons were included if they were more active in a prelude interval before memory-guided saccades to targets presented near the center of their response fields (75 ms interval starting 100 ms before saccade onset) than during an earlier fixation interval (100 ms before fixation target offset) (*S2*,*S3*,*S5*).

Neurons were also tested for maintaining >10 spikes/s while monkeys fixated during the blank interval in the fixation-blink paradigm, and for pausing during large (>10^{o}) ipsiversive and contraversive saccades (*S4*). These two additional criteria helped confirm that the neurons were eye-movement-related, and they were especially useful when it was hard to map the entire "spatial tuning" of the neurons possibly because of the so-called saccade dead zone (*S3*,*S6*).

For comparison, we also examined more caudal SC neurons, representing peripheral locations, and four sample neurons from this group are shown in Fig. S4.

Reversible inactivation. We inactivated portions of the SC of monkeys A and W using local muscimol injections (*S1*) (0.5 μL, 5 μg/μL). Our injections were centered on the intermediate and deep layers of the SC (1.8–2.5 mm below surface) and spanned a range of sites across the SC map in 14 experiments. We inactivated at rostral sites in both monkeys; in monkey W, our second monkey for the inactivation experiments, we also sampled more caudal sites to investigate how more peripheral parts of the SC map might contribute to microsaccade generation. We also injected saline in two control sessions (one per monkey) at sites previously inactivated with muscimol. We identified our inactivated sites as described in detail in (*S1*).

Microsaccade detection and analysis. We recorded eye movements using the electromagnetic induction technique (*S7*,*S8*). Our analysis focused on microsaccades; we did not attempt to detect or analyze the small drifts in eye position that also occur during periods of fixation.

To detect microsaccades, we employed velocity and acceleration thresholds using a method identical to that used by Krauzlis and Miles (*S9*). In this method, the point of peak radial eye velocity (above a threshold parameter, which we initially set to 8 deg/s) was flagged as part of a saccade. Then, flanking regions around this point during which eye velocity remained higher than the velocity threshold were included as part of the same saccade. After that stage, the start and end points of the saccade

being flagged were refined by finding the time points at which eye acceleration in the direction of the saccade exceeded (for saccade start) or went below (for saccade end) a second threshold parameter (the acceleration threshold, which we initially set to 550 deg/s^2). Our choice of velocity and acceleration thresholds was made empirically in order to avoid erroneous flagging of drifts/noise while at the same time accounting for the fact that microsaccades are generally slower than larger voluntary saccades. Even with this choice, there may have been cases in which the algorithm failed. Thus, after running the saccade detection algorithm, we visually inspected every trial and each individual microsaccade, and we manually verified that the algorithm did not erroneously miss a microsaccade or falsely detect one. After all of these steps, we confirmed the accuracy of our detection algorithm and manual inspection by plotting the main sequence curve for microsaccades and comparing it to that of larger saccades (Fig. S1A).

To visualize individual microsaccades as in Fig. 1C, E, G, we temporally realigned the eye movement data so that the zero value on the x-axis corresponded to microsaccade onset. We also corrected for the small differences in absolute eye position prior to microsaccade onset by realigning the y-axis so that all movements had a similar starting position (with small offsets as described in the legend of Fig. 1). This step was necessary for visualizing the microsaccades, because otherwise these extremely small movements were obscured by the differences in starting eye position. This vertical realignment also explains the slight dip that can be noticed for the session in Fig. 1G.

During recording, we detected 282 +/- 90 s.d. microsaccades/session, with an average amplitude of 13.7 min arc +/- 8.5 min arc s.d.. We obtained spike densities (or firing rates) by convolving spike times with a Gaussian of 10 ms s.d.

To obtain firing rate maps like those in Fig. 1B, D, F, we plotted the horizontal (x-axis) and vertical (y-axis) amplitudes of each detected microsaccade and the corresponding neuronal discharge during that particular movement (z-axis; color coded from low to high firing rate). The long fixation trials in our paradigm resulted in many different microsaccades of many different directions and amplitudes, which allowed us to uncover the selectivity of each neuron for subsets of microsaccades. However, we did not have experimental control over individual microsaccades, because these movements are mostly involuntary and because it is hard to test voluntary saccades of this small size (Fig. S1B). Consequently, we found that on occasion, our monkeys exhibited idiosyncratic microsaccade patterns in which certain directions and amplitudes were more prevalent than others. For example, for Neuron c (Fig. 1F), the monkey's pattern of microsaccades was asymmetric, but fortunately the bias in microsaccade generation in that experiment happened to be aligned with the neuron's preferred axis.

To obtain population summaries (Fig. 2A), we binned all microsaccades along a neuron's preferred direction (based on its spatial tuning obtained with the visually-guided saccade task) according to microsaccade amplitude (bin range: 3-30 min arc; bin spacing: 1 min arc; bin width: 5 min arc; minimum number of microsaccades per bin: 5) and direction (contralateral or ipsilateral). We then computed the peak firing

rate of the neuron during microsaccades in each amplitude bin, and normalized based on the bin with peak activity. To study activity observed during larger visually-guided (voluntary) saccades (for example, Fig. 2B), we employed a similar procedure, but the amplitude bin width and spacing for the visually-guided saccades were 1 deg and 1.5-2 deg, respectively.

During inactivation, we analyzed the final 1,000 ms of fixation (before gap onset), to ensure that fixation was stable. We counted the average number of microsaccades per second and compared it to the baseline value. We also measured the frequency of microsaccades after dividing the movements into those directed contralateral to the injected side (contralesional) and those directed ipsilateral. Our choice of analysis epoch avoided confounds associated with acquiring the fixation spot or preparing the visually guided saccade that followed. First, our analysis epoch started well after any transients associated with the beginning of the trial (at least 500 ms after entering the central fixation window). Indeed, because the monkey started the trial by making a saccade from the periphery to the central fixation spot, our analysis interval avoided any transient small saccades that may have been required by the monkey as he was establishing fixation. Second, our analysis epoch ended before gap onset and 200 ms before the appearance of the peripheral saccade target. Thus, our tally of microsaccades was also unlikely to have been influenced by the preparation of future voluntary saccades.

Modeling. Based on previous studies, we assumed that fixation of a small spot recruits a Gaussian profile of SC activity representing this spot's retinotopic location on the SC map (*S1,S2,S10*). For the present simulations, the model SC map represented 0.05-19.55 deg eccentricities on either side, and the activity profile had a standard deviation of 1.06 deg s.d. This value provided a spatial profile of activity across the SC map during fixation that was similar to that observed experimentally (*S2,S10*), but the results from the modeling are not very sensitive to the absolute value of this parameter. The modeled map was one-dimensional, but included both right and left SC, and exhibited logarithmic warping of retinal eccentricities to reflect the SC anatomy (*S11,S12*). We also assumed that each model SC site has an additional noise term with an s.d. of 15% of the average activity at the site (with clipping at 0 and 1 normalized activity). Thus, with 500 iterations of the model, we obtained a baseline distribution of the center of mass of SC activity during fixation of a small foveal target. According to the model, a threshold on this distribution (for example, 2 s.d. from the mean) determined whether an eye movement would be triggered. Also, note that our model assumed that each SC represents only the contralateral visual field. However, the symmetric representation of visual space required by the model is still retained if each of the SC maps extended slightly into the ipsilateral hemifield (as observed experimentally).

We simulated the effects of inactivation by forcing model sites representing 1.55-3.55 deg to have zero activity. We then computed the retinotopic location of the fixation spot that re-establishes equilibrium on average (i.e. that results in a steady-state center of mass of zero; see ref. *S1* for details). With this activity profile, we ran 500 new iterations of the model and compared the resulting center of mass distribution to that without inactivation.

To simulate the effects of peripheral attention, we added to the baseline activity above a Gaussian having 1.2 deg s.d. and centered on 5 deg on the SC map. The amplitude of this added activity was 60% of the normal model activity at the same eccentricities. We then ran 500 iterations of the model, inspecting the resulting distribution of SC activity center of mass.

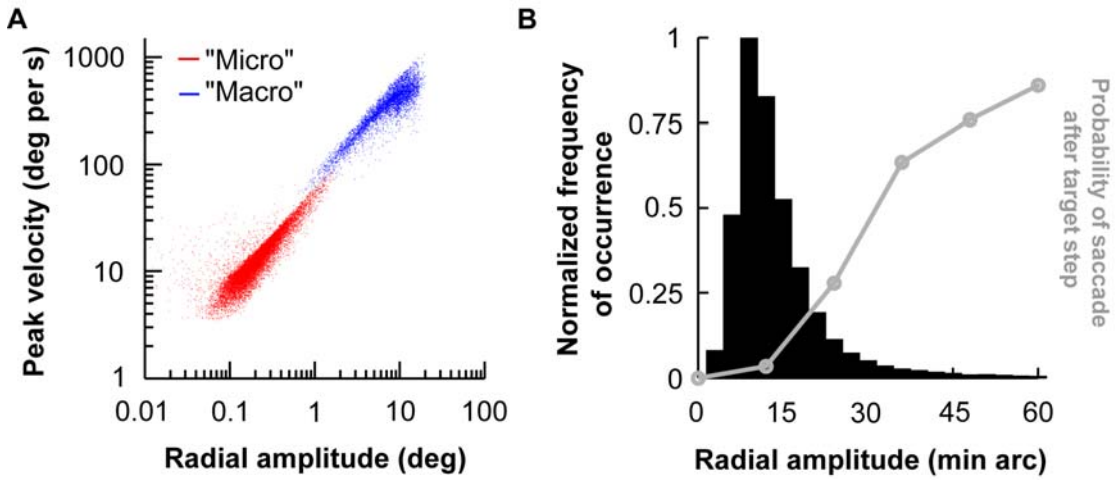

Fig. S1

Behavioral characteristics of microsaccades during fixation. **A,** For all detected microsaccades, we confirmed that these movements had dynamics comparable to those of larger saccades (*S13*). We plotted the peak velocity of the movement against its radial amplitude. Red dots indicate microsaccades during fixation, and blue dots indicate larger voluntary saccades obtained from a visually-guided saccade task. Microsaccades fell on the "main sequence" curve for larger saccades – except that they were much smaller and only caused retinal image translations of ~13.7 min arc +/- 8.5 s.d. **B,** Histogram of the microsaccade amplitudes observed in our experiments (black). The majority of the movements that we studied were less than 30 min arc. The gray curve relates these microsaccade amplitudes to those associated with a frequent observation of increased difficulty in instructing subjects to generate small, target-driven saccades (*S3*,*S6*). Because of this increased difficulty (especially for saccades less than ~30 min arc) (*S3*,*S6*), studies of small microsaccades using tasks common in investigating large saccades can be extremely inefficient. By analyzing SC activity during long fixation trials with plenty of microsaccades, we were able to avoid this difficulty and uncover microsaccade-related activity in the SC even for the tiniest movements. The gray curve was obtained from (*S3*).

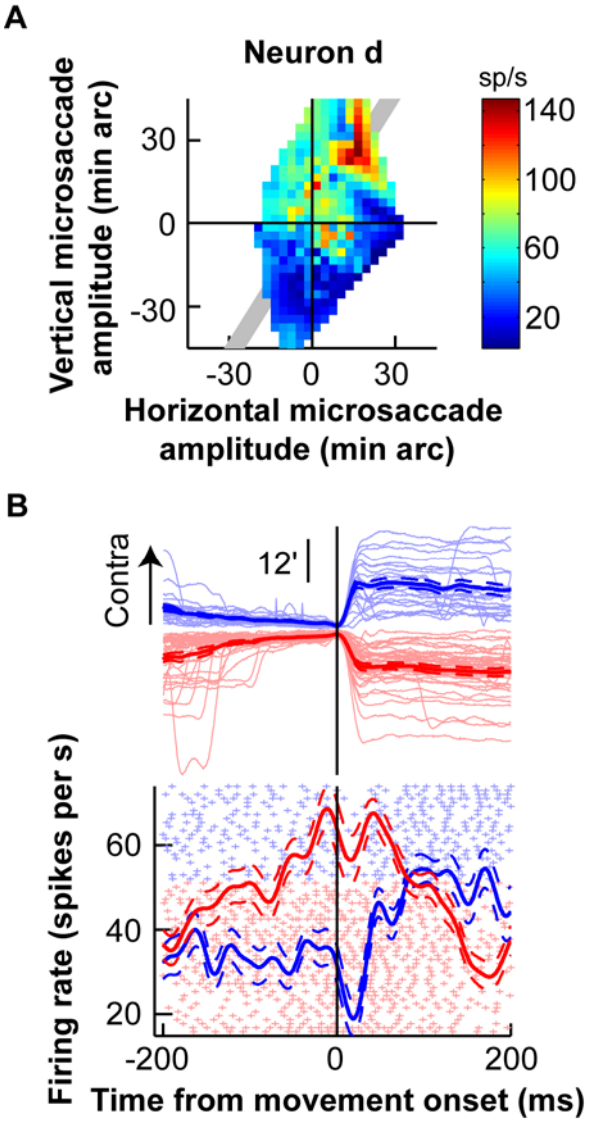

Fig. S2
A sample SC neuron exhibiting preference for ipsilateral microsaccades. **A,** Response field map of the neuron labeled "Neuron d" in Fig. 2A. This neuron was recorded from the right SC. During microsaccades, the neuron exhibited clear preference for ipsilateral movements toward the upper right quadrant. **B,** The raw activity of the neuron for microsaccades within the shaded gray region in **A** shows buildup of activity before the preferred movements just like our other sample neurons in the main text, except that these preferred movements were now ipsilateral. Dashed lines indicate s.e.m. envelopes, and the figure is organized as Fig. 1.

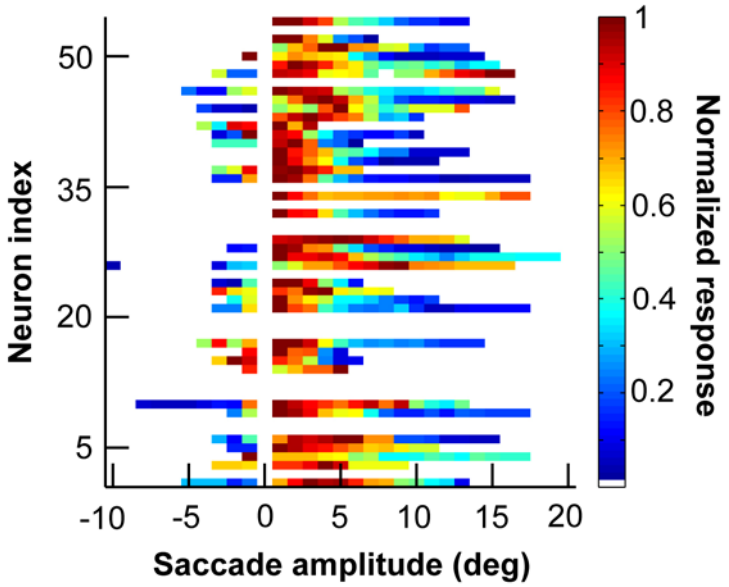

Fig. S3
Behavior of rostral SC neurons during larger “macro” saccades. We performed an analysis similar to that of Fig. 2A but for saccades obtained from a visually-guided saccade task, instead of for microsaccades during fixation. The bulk of the neuronal activity during this task was associated with saccades smaller than ~5 deg. Missing neurons (white space, N = 15) indicate a lack of clear preference for the visually-guided saccades that were sampled in these experiments (for example, reductions or pauses in activity for all tested saccade amplitudes).

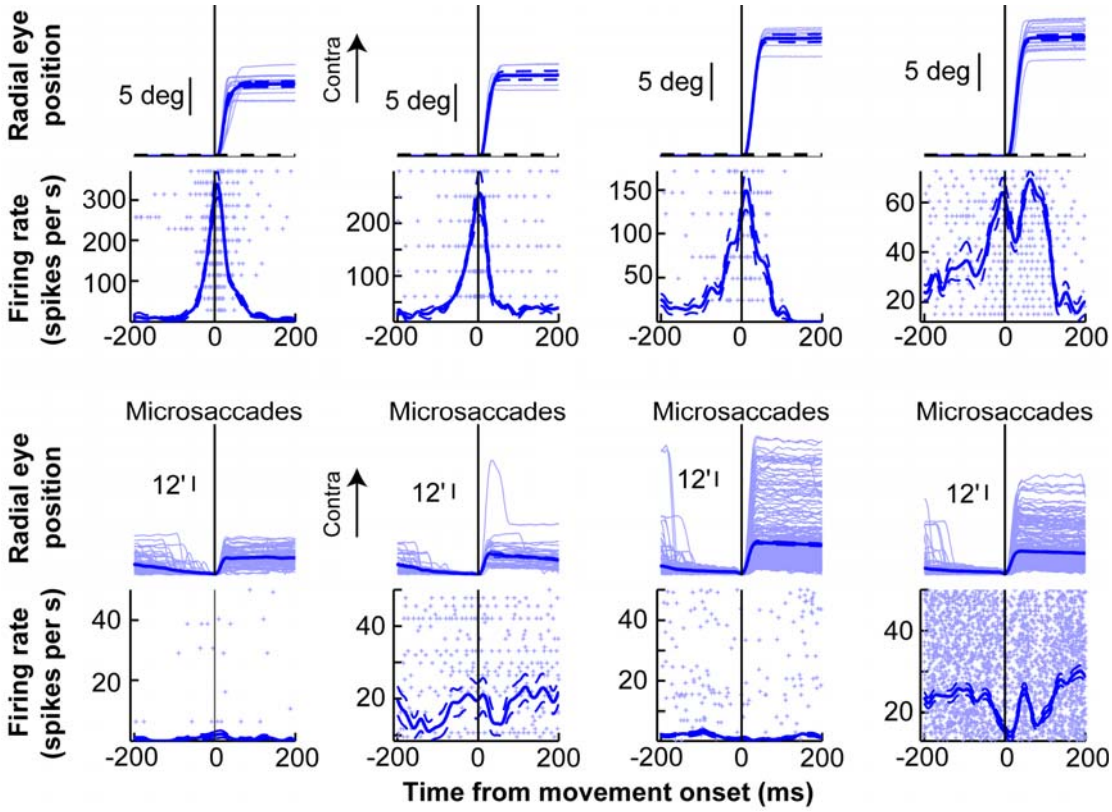

Fig. S4

Lack of microsaccade-related activity from SC neurons preferring peripheral locations. To further test the specificity of microsaccade-related activity, we also recorded from neurons that were spatially tuned for peripheral target locations (mean preferred eccentricity 10 deg +/- 3.4 deg s.d.). This figure shows the spiking activity of four such neurons during large contralateral saccades (upper row of radial eye position and firing rate traces) as well as during contralateral microsaccades occurring while the monkeys fixated a stationary spot (lower row of radial eye position and firing rate traces). Note the different eye position scale bars for the upper and lower rows. To further clarify this difference, the upper eye position traces show a black, horizontal dashed line, which indicates the median radial amplitude of microsaccades obtained during the fixation trials. Each column shows results from one neuron, and the light colors indicate individual eye position traces or individual movement spike rasters. The blue traces with s.e.m. envelopes (as dashed lines) indicate average radial eye position or average firing rate. Note how these four sample neurons show results that are the exact complement of the results obtained from our population of central SC neurons described in the main text. These results further illustrate the response selectivity of individual rostral SC neurons for a particular range of microsaccade amplitudes and directions. Also note that for the fourth neuron, there was a much larger number of microsaccades than large saccades, explaining why the spike raster in the bottom panel appears to have a high density of action potentials. For each neuron, the spike density function (solid firing rate curve), exhibited lower activity during microsaccades than during larger voluntary saccades.

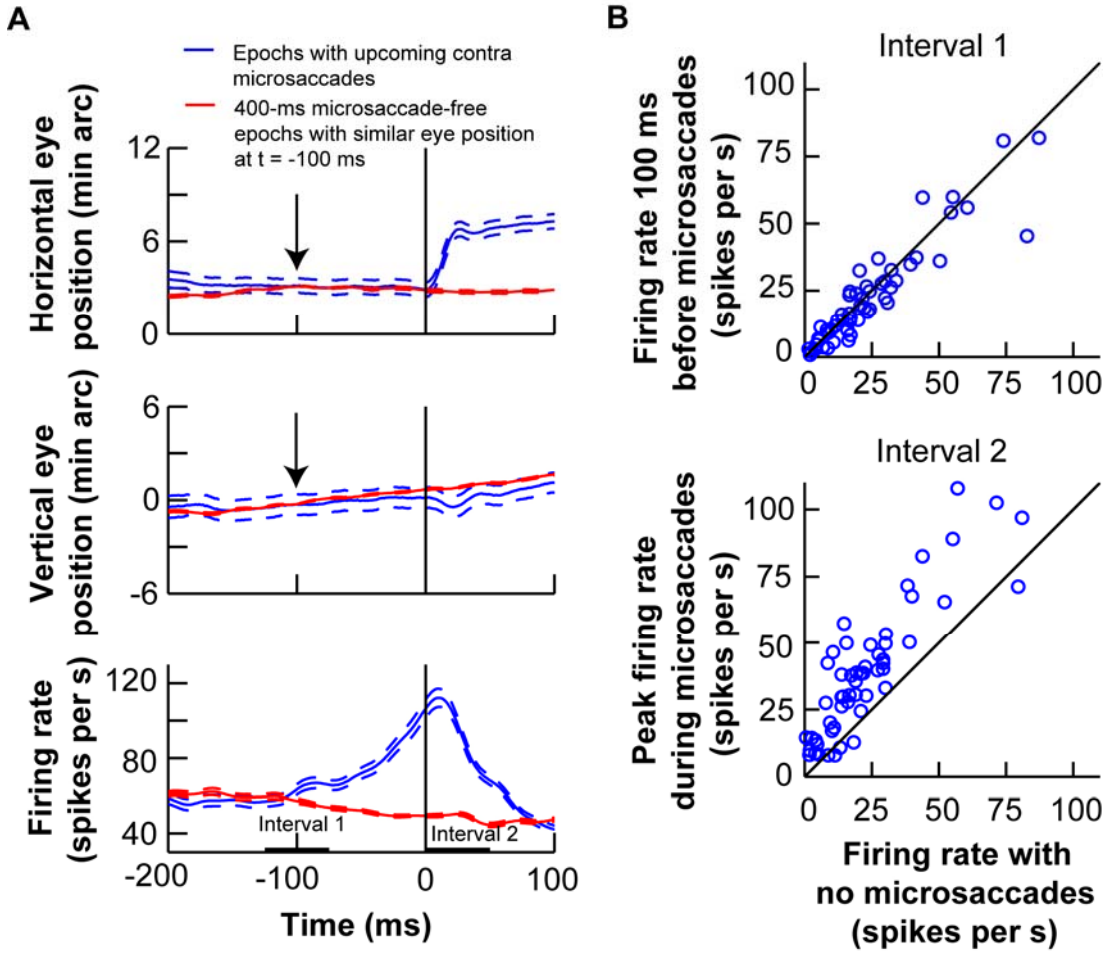

Fig. S5

Microsaccade-related activity after controlling for small eye position deviations before movement onset. **A,** For a sample neuron, we plotted average eye position (blue, top two panels) and average firing rate (blue, bottom panel) but only for contralateral microsaccades having a starting eye position (defined as the position 100 ms before movement onset) that was of a representative value for the session (arrows). We then searched for all 400-ms microsaccade-free epochs having an eye position at the center of these epochs that was within 0.6 min arc of the above starting position. For the same neuron, the average eye position and average firing rate from these microsaccade-free epochs are shown in red (centered on t = -100 ms). With similar eye positions well before microsaccade onset, the neuron had similar activity either with or without an upcoming contralateral microsaccade. However, the activity of the neuron during microsaccades was significantly stronger than its activity without. This is consistent with our observations of increases in SC activity before and during microsaccades that were synchronized with movement onset. Thin dashed lines indicate s.e.m. envelopes. **B,** We summarized this observation across our population of neurons (N = 54) as follows. For each detected contralateral microsaccade (of any amplitude, regardless of neuronal preference), we measured neuronal activity 100 ms before microsaccade onset. We then compared this activity to activity recorded from the microsaccade-free epochs as obtained above (Interval 1

in the bottom of **A**). The top scatter plot indicates that the firing rates were very similar in these two cases ($p = 0.67$, two-tailed t-test across neurons). This is expected because the similar eye positions meant that the retinotopic location of the fixation spot was similar (*S3,S14*). We then measured neuronal activity during microsaccades as well as activity in a similar time frame (and with similar starting eye position) but without microsaccades from the same 400-ms microsaccade-free fixation epochs (Interval 2 in the bottom of **A**). The majority of our neurons were more active during microsaccades ($p < 0.0005$, two-tailed t-test across neurons). Thus, the neuronal modulations that we observed were distinct from modulations based on small eye position deviations from the fixated goal (*S3,S14*).

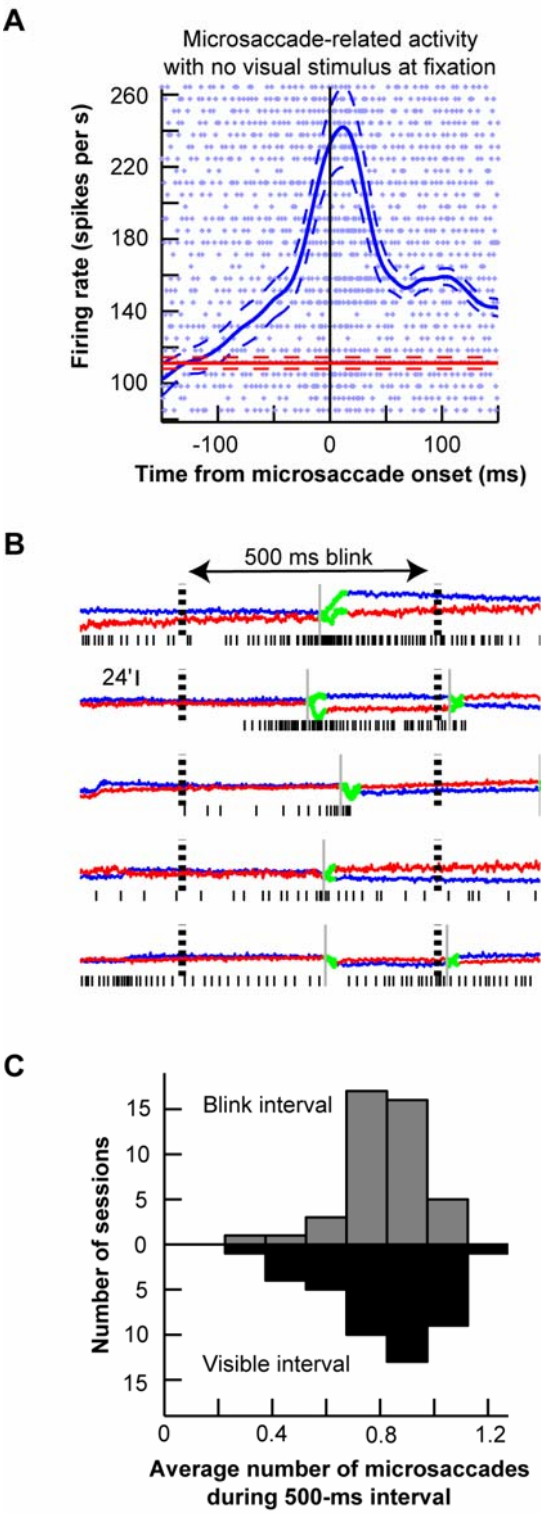

Fig. S6
Independence of microsaccade-related SC activity from the presence of a visual stimulus at fixation. We tested our neurons with a fixation-blink paradigm in which the monkeys maintained steady fixation while we blinked off the fixation spot for 500 ms. **A,** Activity of a sample neuron during microsaccades that occurred inside the

blink interval. We recorded 41 trials of the fixation-blink condition from this neuron. In these trials, the monkey generated 28 microsaccades inside the blink interval. The firing rate is shown (solid blue curve with s.e.m. envelopes) aligned on microsaccade onset for all of these 28 microsaccades (mean amplitude 19.5 min arc +/- 9.7 min arc s.d.). The individual spike rasters (light blue dots) for each movement are also shown. This neuron preferred both contralateral and ipsilateral microsaccades, which allowed us to group all 28 movements in this analysis. As can be seen, the neuron exhibited increases in firing rate that were similar to those observed in our population of neurons (Fig. 1). To further test whether this activity was related to the generation of microsaccades, we calculated the average firing rate during the entire 500-ms blink interval, but after excluding any activity occurring from 100 ms prior to microsaccade onset until 50 ms after microsaccade offset. This average firing rate (depicted by the horizontal red line) was significantly lower than the firing rate leading up to microsaccades. Thin dashed lines indicate s.e.m. envelopes. **B,** Individual trials from the fixation-blink condition for five sample neurons from our population. The region between the thick dashed lines indicates the interval during which the fixation spot was not visible. The top row of eye positions and spike rasters shows a sample trial from the neuron in **A**. Each of the remaining rows shows a trial from a different sample neuron illustrating microsaccades during the blink interval that were in the preferred direction of the neuron (or anti-preferred for the fifth sample neuron). Because of the selectivity of neurons for certain microsaccade directions and amplitudes (Fig. 1, 2), not every blink trial contained microsaccades in the preferred (or anti-preferred) directions. However, as can be seen, when they did occur, such microsaccades were associated with neuronal modulations similar to those observed in our main experiment and in **A**. Also, note that later microsaccades that occurred after fixation spot reappearance also caused modulation consistent with the neuron's selectivity. For example, for the fifth sample neuron, the microsaccade during the blink was not preferred by the neuron and was associated with a pause in activity, but the microsaccade directly after it was in the preferred direction and was associated with an increase in activity. Other details of this panel are like Fig. 1A. **C,** Microsaccades occurred in the absence of a visual fixation spot, providing an explanation for the independence of SC microsaccade-related activity from the visual stimulus (**A**, **B**). We measured the average number of microsaccades occurring during the 500-ms blink interval in the fixation-blink paradigm and compared it to the average number of microsaccades in an identical epoch immediately following this interval, in which the fixation spot was visible and the monkey was still required to maintain fixation. Across sessions, there was no significant difference in the frequency of occurrence of microsaccades between the two epochs ($p = 0.91$, two-tailed t-test across sessions).

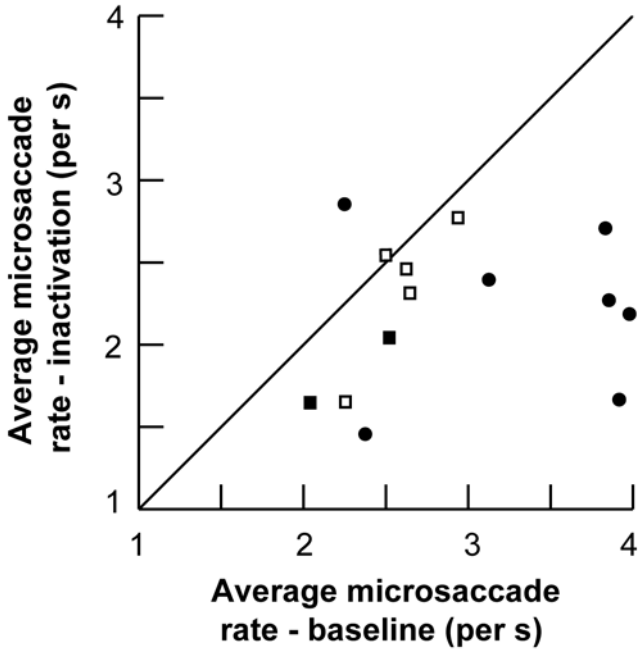

Fig. S7
Average microsaccade rates before and after SC inactivation. This figure shows the same data as in Fig. 3B (N = 14), but in a form that illustrates absolute rate values instead of changes in rate. The filled symbols indicate experiments in which the inactivation rates were significantly different from the baseline rates ($p < 0.05$, ranksum test, N = 48 trials for baseline and N = 48 trials for inactivation). Circles indicate experiments with monkey A; squares indicate experiments with monkey W. The majority of experiments resulted in reduced microsaccade occurrences during fixation. The experiments with no change in rate were mostly ones in which the inactivation targeted peripheral SC sites, as shown in Fig. 3B; these experiments were more frequent in monkey W.

References

S1. Z. M. Hafed, L. Goffart, R. J. Krauzlis, *J. Neurosci.* **28**, 8124-8137 (2008).

S2. Z. M. Hafed, R. J. Krauzlis, *J. Neurosci.* **28**, 9426-9439 (2008).

S3. R. J. Krauzlis, M. A. Basso, R. H. Wurtz, *J. Neurophysiol.* **84**, 876-891 (2000).

S4. D. P. Munoz, R. H. Wurtz, *J. Neurophysiol.* **70**, 559-575 (1993).

S5. R. J. Krauzlis, *J. Neurosci.* 23: 4333-4344 (2003).

S6. C. Rashbass, *J. Physiol.* **159**, 326-338 (1961).

S7. S. J. Judge, B. J. Richmond, F. C. Chu, *Vision Res*. **20**, 535-538 (1980).

S8. A. F. Fuchs, D. A. Robinson, *J. Appl. Physiol.* **21**,1068-1070 (1966).

S9. R. J. Krauzlis, F. A. Miles, *J. Neurophysiol.* **76**, 2822-2833 (1996).

S10. D. P. Munoz, R. H. Wurtz, *J. Neurophysiol.* **73**, 2334-2348 (1995).

S11. F. P. Ottes, J. A. Van Gisbergen, J. J. Eggermont, *Vision Res.* **26**, 857-873 (1986).

S12. C. Quaia, H. Aizawa, L. M. Optican, R. H. Wurtz, *J. Neurophysiol.* **79**, 2097-2110 (1998).

S13. B. L. Zuber, L. Stark, G. Cook, *Science* **150**, 1459-1460 (1965).

S14. R. J. Krauzlis, M. A. Basso, R. H. Wurtz, *Science* **276**, 1693-1695 (1997).